Analysis of BOD, COD concentration level by mathematical model

Priti V. Tandel[1]
Department of Mathematics,
Veer Narmad South Gujarat University, Surat, Gujarat, India
pvtandel@vnsgu.ac.in

Manan A. Maisuria[2]
Department of Mathematics,
Veer Narmad South Gujarat University, Surat, Gujarat, India.
mananmaisuria.maths21@vnsgu.ac.in

Abstract:
This research aims to investigate the use of mathematical models to analyze the diffusion and transport of chemicals in river systems. This work presents a one-dimensional model characterized by a time-dependent advection diffusion equation. In addition, we have used the reduced differential transform method (RDTM) to solve these models. To verify the model, we researched the diffusion and transportation of chemicals, with a special emphasis on BOD (Biochemical Oxygen Demand) and COD (Chemical Oxygen Demand). Our research aims to determine the possible levels of biochemical oxygen demand (BOD) and chemical oxygen demand (COD) in the Tapi River, without any identifiable pollution source. The present analysis seeks to examine the impact of velocity on the BOD and COD profiles of the Tapi River. Numerical and graphical representations have shown the effect of velocity changes on BOD and COD concentration profiles at different distances. To evaluate the quality and precision of the solution, we get the exact general solution function for each case, which has been derived via RDTM. Numerical and graphical representations have been used to demonstrate the concentration of BOD and COD at different distances and time intervals. The methods suggested in this paper for predicting the levels of BOD and COD in rivers using a 1D pollution model can also be used for other rivers.

1 Introduction

In this time of quick development and fast advancement of civilization, ecology and environmental preservation are gaining growing significance. The environment impacts humanity, and in turn, humanity likewise exerts an impact on the habitat it inhabits, but often in a detrimental manner. Nevertheless, a significant portion of this unsuitable behavior may be eradicated by adopting an eco-conscious mindset. Water is one of the several variables that influence the degree of civilization. The demands for water quality are always rising, necessitating ongoing water purity assessments. As a consequence, there has been a development and adoption of highly effective and sometimes unorthodox manufacturing methods that safeguard the environment. Water exhibits continuous movement, traversing terrestrial surfaces, the atmosphere, and the world's seas. Rivers are crucial components of water management and serve as a renewable fresh water reservoir. The introduction of many biological and chemical substances into the environment has resulted in alterations to the water quality (Al Jibouri, 2018; Beveridge, 2020). Primarily, we people provide a significant threat to this invaluable resource. Water pollution is a significant issue that has a direct impact on human life, the survival of fish, and overall environmental health. Consequently, several efforts are undertaken to seek out cost-effective, efficient, and eco-friendly water systems (Raafat, 2023).

An analytical solution is obtained for two dispersion issues by using a Laplace transformation approach to a linear advection-diffusion equation with variable coefficients in a one-dimensional semi-infinite medium (Jaiswal, 2009) . The authors investigated the problem of pollution movement by using a mathematical model based on the one-dimensional advection-dispersion equation. This model incorporates factors such as decay and expansion processes via Laplace transformation. To get numerical answers, the authors used the finite difference approach (Manitcharoen, 2020) . The Laplace integral transformation method (LITT) is used to derive an analytical solution for the two-dimensional advection-dispersion equation with variable coefficients in a semi-infinite heterogeneous porous medium (Yadav, 2021) . The one-dimensional ADE depicting exponential fluctuations in pollutant concentration was solved numerically and analytically by the authors, who also recorded the findings with respect to the clean-water release remediation of pollution (Saleh, 2022).

The main objective of this work is to study the time-dependent transport of substances in a water medium during the eutrophication process by thoroughly integrating multiple components, including mathematical modeling, transformation methods, approximations, and computer implementation. The initial data that was gathered makes applying the suggested mathematical models and techniques simple. The created model provides a quick and efficient way to evaluate the water quality in river systems. Moreover, this idea may be applied to other fields of science and engineering. A model has been created to examine the dispersion of pollutants in rivers.

The current investigation involves collecting water samples from the Tapi river in Surat, India. The purpose is to create a mathematical model that can forecast pollution levels at various distances and times. This work presents a mathematical model that describes the movement of pollutants in one dimension. The reduced differential transform method (RDTM) is used in order to solve the governing equation, which is a one-dimensional advection-diffusion equation. In addition to this, we have investigated the convergence of analytical solutions obtained by the RDTM method.

The mathematical expression for the problem is explicated in Section 3. A detailed summary of the foundational principles that form the basis of the RDTM is provided in Section 4. As part of an evaluation of the method's efficacy, Section 5 examines the numerical results and convergence. A graphical representation of the obtained solutions is generated through the application of 2D and 3D plots. The conclusion is succinctly summarized in Section 6.

2 Water Sample Collection

Figure 1 about here

This study investigates the Tapi River in Surat, from the Pal-Umra bridge to the ONGC bridge. On November 12, 2022, seven samples with a 1 Litre capacity were collected in similarly sized bottles from the start of the research area. The concentrations of BOD and COD were examined using these water samples. The collected data was sent to Pollucon Laboratories Pvt. Ltd., located in Navjivan Circle, Surat, Gujarat, for the purpose of determining BOD and COD. A few images of the research region are shown in Figure 1. The initial concentrations of BOD and COD in the study region are shown numerically in Table 1.

Table 1 about here

3 Mathematical Formulation of the problem

Pollutant tracer particles or insoluble solutes are a major contributor to the degradation of the hydro-environment in aquifers and surface water bodies. It is possible to link the causes of these pollutants to human activity on Earth's surface. Wastewater drainage carries solute particles to surface water bodies, where they seep into aquifers. Mines, underground septic tanks, waste disposal sites, and polluted water sources that refill the aquifers are the causes of this intrusion. Diffusion and advection work together to spread out the solutes as the flow moves downstream. An advection-diffusion equation, a partial differential equation of the parabolic type, may be used to quantitatively simulate the phenomena of concentration drop across time and space. Environmentalists, hydrologists, civil engineers, and mathematical modelers have all shown a great deal of interest in the advection-diffusion equation as their worries about the safe hydro-environment required for life on Earth grow (Dilip Kumar, 2011). Mathematically, the advection-diffusion equation in one dimension can be expressed as a second-order parabolic partial differential equation. It can be represented as:

$$A\frac{\partial c}{\partial T} = \frac{\partial}{\partial X}\left(AD\frac{\partial c}{\partial X}\right) - Av^{*}\frac{\partial c}{\partial X} + Af \qquad (1)$$

where $c\,(mg/L)$ is the BOD or COD concentration throughout its path through the medium along the flow field at any given time $T\,(hour)$ and distance $X\,(km)$. The Longitudinal Diffusion coefficient is expressed as $D\,(km^2/hour)$. The irregular uniform seepage flow velocity in the longitudinal direction is expressed as $v^* \ (km/hour)$. The flow area of a river's cross-section is $A\,(km^2)$. $f\ (mg/km^3 hour)$ is a source term. X is the longitudinal distance from the study area's beginning. The dimension of time is T. Throughout the investigation, the cross-sectional area of the river is considered a constant. Equation (1) then transforms into the following form:

$$\frac{\partial c}{\partial T} = \frac{\partial}{\partial X}\left(D\frac{\partial c}{\partial X}\right) - v^* \frac{\partial c}{\partial X} + f \tag{2}$$

The description of the dimensionless variables is given as (Rubbab, 2016):

$$x = \frac{X}{L},\ t = \frac{DT}{L^2},\ v = \frac{v^* L}{D},\ S = \frac{L^2 f}{D} \tag{3}$$

L represents the length of the research section of the river. We obtain a dimensionless advection-diffusion equation in the given form.

$$\frac{\partial c}{\partial t} = \frac{\partial^2 c}{\partial x^2} - v\frac{\partial c}{\partial x} + S \tag{4}$$

To examine this problem, we have utilized the levels of BOD and COD in the Tapi River. This report focuses on a research region of 5 kilometers along the Tapi River, specifically from the ONGC bridge to the Pal Umra bridge. It is assumed that there is no any pollutant source in research area. So, we take $S = 0$ in this paper. The length of the river, shown as L, is 5 kilometers. Based on data collected on the concentration of BOD and COD at a specific period $t = 0$, the concentration is fitted in the following form with favorable statistical indicators.

Table 2 about here

Figure 2 about here

Figure 3 about here

Figures 2 and 3 illustrate the process of curve fitting for the initial equation, particularly for BOD and COD, respectively, by graph. Table 2 presents the goodness of fit results corresponding to BOD and COD initial conditions. Therefore, we are given the initial function equations (5) and (6) for BOD and COD correspondingly.

BOD initial function: $c(x,0) = 2.17\ x^4 - 20.89\ x^3 + 61.3\ x^2 - 35.56\ x + 64.29$ (5)

COD initial function: $c(x,0) = 7.491\ x^4 - 71.83\ x^3 + 209.4\ x^2 - 116.2\ x + 231.8$ (6)

4 Reduced Differential Transform Method

Let $b(\xi,\tau)$ be a two-variable function. Assume that $b(\xi,\tau)$ can be described as the combination of two single variable functions. i.e., $b(\xi,\tau) = k(\xi)l(\tau)$

By properties of differential transform, $b(\xi,\tau)$ can be represented as

$$b(\xi,\tau) = \sum_{i=0}^{\infty} M_{(i)}\xi^i \sum_{j=0}^{\infty} L_{(j)}\tau^j = \sum_{k=0}^{\infty} B_k(\xi)\tau^k$$

Where $B_k(\tau)$ is called t-dimensional spectrum function of $b(\xi,\tau)$ (Al-Amr, 2014).

$$B_k(\xi) = \frac{1}{k!}\left[\frac{\partial^k}{\partial \tau^k} b(\xi,\tau)\right]_{\tau=0} \tag{7}$$

In this paper, Uppercase letters $[B(\xi,\tau)]$ denote changed functions, whereas lowercase letters $[b(\xi,\tau)]$ denote original functions. The differential inverse transform of $B_k(\xi)$ is defined by

$$b(\xi,\tau)=\sum_{k=0}^{\infty}B_k(\xi)\tau^k \tag{8}$$

From Equations (7) and (8) We get

$$b(\xi,\tau)=\sum_{k=0}^{\infty}\frac{1}{k!}\left[\frac{\partial^k}{\partial\tau^k}b(\xi,\tau)\right]_{\tau=0}\tau^k \tag{9}$$

Basic concept of RDTM, Consider the nonlinear differential partial differential equation:

$$Lb(\xi,\tau)+Rb(\xi,\tau)+Nb(\xi,\tau)=\vartheta(\xi,\tau) \tag{10}$$

with the initial condition $b(\xi,0)=y(x)$,

where $L=\frac{\partial}{\partial t}$, $Rb(\xi,\tau)$ is a linear operator which has partial derivatives, $Nb(\xi,\tau)$ is a nonlinear term and $\vartheta(\xi,\tau)$ is an inhomogeneous term.

By applying the transform on equation (10), we get

$$(k+1)B_{k+1}(\xi)=\psi_k(\xi)-RB_k(\xi)-NB_k(\xi) \tag{11}$$

where $B_k(\xi),\psi_k(\xi),RB_k(\xi)$ and $NB_k(\xi)$ are transform of $b(\xi,\tau),\vartheta(\xi,\tau),Rb(\xi,\tau)$ and $Nb(\xi,\tau)$ respectively. from initial condition, we can write

$$B_0(x)=y(x) \tag{12}$$

By solving equations (11) and (12), we get the values of $B_k(\xi)$. Subsequently, an estimated solution is generated by performing an inverse transformation on the collection of values $\{B_k(\xi)\}_{k=0}^{n}$. The result of this transformation is an approximate answer.

$$\tilde{b}_n(\xi,\tau)=\sum_{k=0}^{n}B_k(\xi)\tau^k \tag{13}$$

where n is an approximation order solution. Hence, the exact solution to the problem is stated by

$$b(\xi,\tau)=\lim_{n\to\infty}\tilde{b}_n(\xi,\tau). \tag{14}$$

Table 3 about here

5 Results and discussion

5.1 BOD concentration

Using RDTM to solve equation (4) with BOD initial condition (5). We get

$c(x,t)=M_0+M_1t+M_2t^2+M_3t^3+M_4t^4+\dots$

where

$M_0=2.17\,x^4-20.89\,x^3+61.3\,x^2-35.56\,x+64.29$

$$M_1=\frac{651x^2}{25}-v\left(\frac{217x^3}{25}-\frac{6267x^2}{100}+\frac{613x}{5}-\frac{889}{25}\right)-\frac{6267x}{50}+\frac{613}{5}$$

$$M_2 = \frac{651v^2x^2}{50} - \frac{6267v^2x}{100} + \frac{613v^2}{10} - \frac{1302vx}{25} + \frac{6267v}{50} + \frac{651}{25}$$

$$M_3 = \frac{v^2(2089v - 868vx + 2604)}{100}$$

$$M_4 = \frac{217v^4}{100}$$

Given general series solution of BOD concentration function is exact solution.

Table 4 about here

Figure 4 about here

Figure 5 about here

Figure 6 about here

The numerical values of the BOD concentration obtained at various x and t are shown in Table 4. The three-dimensional graphical depiction of the BOD concentration is shown in Figure 4. Both Figure 5 and Figure 6 provide a visual depiction of BOD in two dimensions, with fixed t and x being used as fixed variables, respectively. As the value of the variable t increases, we found that the value of BOD also increases. In addition, the value of BOD continues to drop as the value of variable x continues to rise.

Table 5 about here

Figure 7 about here

The numerical values of BOD for various values of v and fixed $t = 0.5$ are provided in Table 5. The graphic depiction of the impact of a variation in v on the profile of BOD concentration is shown in Figure 7. In this case, we found that the increase in BOD value and the rise in v value were positively correlated.

5.2 COD concentration

Using RDTM to solve equation (4) with COD initial equation (6). We get

$c(x,t) = A_0 + A_1t + A_2t^2 + A_3t^3 + A_4t^4 + \ldots$

where

$A_0 = 7.491\,x^4 - 71.83\,x^3 + 209.4\,x^2 - 116.2\,x + 231.8$

$$A_1 = \frac{22473x^2}{250} - v\left(\frac{7491x^3}{250} - \frac{21549x^2}{100} + \frac{2094x}{5} - \frac{581}{5}\right) - \frac{21549x}{50} + \frac{2094}{5}$$

$$A_2 = \frac{22473v^2x^2}{500} - \frac{21549v^2x}{100} + \frac{1047v^2}{5} - \frac{22473vx}{125} + \frac{21549v}{50} + \frac{22473}{250}$$

$$A_3 = \frac{11v^2(3265v - 1362vx + 4086)}{500}$$

$$A_4 = \frac{7491v^4}{1000}$$

Given general series solution of COD concentration function is exact solution.

Table 6 about here

Figure 8 about here

Figure 9 about here

Figure 10 about here

Table 6 presents the numerical values of the COD concentration obtained at different values of x and t. Figure 8 illustrates the three-dimensional graphical representation of the concentration of COD. COD profile is illustrated visually in two dimensions in both Figure 9 and Figure 10, where t and x are designated as fixed variables, respectively. It was observed that as the value of the variable t increases, so does the value of COD. Furthermore, as the value of variable x increases, the value of COD continues to decrease.

Table 7 about here

Figure 11 about here

Table 7 presents the COD concentration numerical values for different values of v, with a fixed $t = 0.5$. Figure 11 illustrates the graphical representation of how a change in v affects the profile of COD concentration. Here, we observed a positive correlation between the rise in the value of v and the increase in the value of COD.

6 Conclusion

This work presents an extensive mathematical model that explores several methods for predicting river chemical concentrations. We get the initial condition by collecting data on BOD and COD in the most optimal format, yielding favorable statistical indicators. We have obtained two distinct solutions for BOD and COD. It can be determined that the concentration of BOD and COD increases with an increase in time. The concentration of BOD and COD decreases with an increase in the length of river. During the monsoon season, it is evident that the velocity of the river is heightened. This article also examines the impact of variations in river velocity on the profiles of BOD and COD concentrations. Increasing the river's velocity leads to a corresponding rise in the values of BOD and COD. The primary advantage of the RDTM is its ability to provide the user with a rapidly converging power series representation that includes accurately computed components, hence offering an analytical approximation and often an exact solution in many situations. When employing RDTM, there are no discretization or inescapable presumptions. At times, RDTM surpasses methods such as DTM. Moreover, if physically identifiable areas with high pollution levels can be found, the study methodology might provide a valuable approach for achieving cost-effective watershed management. The suggested technique enables the effective design of river state estimate control for actual systems. This study offers a valuable instrument for researchers to analyze and differentiate the effectiveness of various models, resulting in compelling and applicable findings. It is feasible to expand this study to include the analysis of the two-dimensional advection-diffusion equation.

Acknowledgement

Priti V. Tandel is thankful to Veer Narmad South Gujarat University, Surat for providing the opportunity to undertake the minor project. This research is conducted as a part of a minor project at Veer Narmad South Gujarat University, Surat and the experience gained has been invaluable to academic and professional development.

References

Al Jibouri, A. K. H., Upreti, S. R., & Wu, J. (2018). Optimal control of continuous ozonation of non-biodegradable pollutants. Journal of Process Control, 66, 1-11.

Al-Amr, M. O. (2014). New applications of reduced differential transform method. Alexandria Engineering Journal, 53(1), 243-247.

Beveridge, C., Hossain, F., Biswas, R. K., Haque, A. A., Ahmad, S. K., Biswas, N. K., ... & Bhuyan, M. A. (2020). Stakeholder-driven development of a cloud-based, satellite remote sensing tool to monitor suspended sediment concentrations in major Bangladesh rivers. *Environmental Modelling & Software*, *133*, 104843.

Dilip Kumar, J., Atul, K., & Raja Ram, Y. (2011). Analytical solution to the one-dimensional advection-diffusion equation with temporally dependent coefficients. Journal of Water Resource and Protection, 2011.

Jaiswal, D. K., Kumar, A., Kumar, N., & Yadav, R. R. (2009). Analytical solutions for temporally and spatially dependent solute dispersion of pulse type input concentration in one-dimensional semi-infinite media. *Journal of Hydro-environment Research*, *2*(4), 254-263.

Maisuria, M. A., & Tandel, P. V. (2023). Mathematical modelling and application of reduced differential transform method for river pollution. Ratio Mathematica, 47.

Manitcharoen, N., & Pimpunchat, B. (2020). Analytical and numerical solutions of pollution concentration with uniformly and exponentially increasing forms of sources. Journal of Applied Mathematics, 2020, 1-9.

Raafat, P. B., Ibrahim, F. N., & Saleh, A. (2023). On determining conditions and suitable locations for fish survival by using the solution of the two coupled pollution and aeration equations. *Scientific Reports*, *13*(1), 6560.

Rubbab, Q., Mirza, I. A., & Qureshi, M. (2016). Analytical solutions to the fractional advection-diffusion equation with time-dependent pulses on the boundary. AIP Advances, 6(7).

Saleh, A., Ibrahim, F. N., & Hadhouda, M. K. (2022). Remediation of pollution in a river by releasing clean water. Inf. Sci. Lett, 11, 127-133.

Srivastava, V. K., Awasthi, M. K., & Kumar, S. (2014). Analytical approximations of two and three dimensional time-fractional telegraphic equation by reduced differential transform method. Egyptian Journal of Basic and Applied Sciences, 1(1), 60-66.

Yadav, R. R., & Kumar, L. K. (2021). Analytical solution of two-dimensional conservative solute transport in a heterogeneous porous medium for varying input point source. Environmental Earth Sciences, 80, 1-10.

Table 1: BOD and COD at initial time

Samle No.	$x\ (km)$	BOD $(mg\,/\,L)$	COD $(mg\,/\,L)$
1	0	64	230
2	0.5	61	225
3	1	68	250
4	1.5	92	330
6	2.5	116	420
8	3.5	121	435
11	5	164	590

Table 2: Statistical data of curve fitting

Goodness of fit				
Concentration	SSE	R-square	Adjusted R-square	RMSE
BOD	21.55	0.9975	0.9925	3.283
COD	206.8	0.9981	0.9944	10.17

Table 3: Reduced differential transformation (Keskin, 2010; Maisuria M. A., 2023; Srivastava, 2014)

Original form	Transformed form
$b(\xi,\tau)$	$B_k(\xi)=\frac{1}{k!}\left[\frac{\partial^k}{\partial\tau^k}b(\xi,\tau)\right]_{\tau=0}$
$\alpha\, p(\xi,\tau)\pm\beta q(\xi,\tau)$	$\alpha P_k(\xi)\pm\beta Q_k(\xi)$
$\xi^m\tau^n$	$\xi^m\delta(k-n)$
$\xi^m\tau^n b(\xi,\tau)$	$\xi^m B_{k-n}(\xi)$
$z(\xi,\tau)=p(\xi,\tau)q(\xi,\tau)$	$Z_k(\xi)=\sum_{r=0}^{k}P_r(\xi)Q_{k-r}(\xi)$
$\frac{\partial^r}{\partial\tau^r}b(\xi,\tau)$	$\frac{(k+r)!}{k!}B_{k+r}(\xi)$
$\frac{\partial}{\partial\xi}b(\xi,\tau)$	$\frac{\partial}{\partial\xi}B_k(\xi)$

Table 4: Numerical value of BOD at different x and t for $v=0.5$

$x\setminus t$	0.1	0.2	0.3	0.4	0.5	0.6	0.7	0.8	0.9	1
0.1	74.5629	89.8516	107.247	126.804	148.578	172.625	198.999	227.759	258.959	292.657
0.2	70.9647	84.4332	99.9257	117.496	137.2	159.091	183.225	209.658	238.445	269.642
0.3	68.463	80.2227	93.9249	109.623	127.372	147.224	169.236	193.461	219.955	248.774
0.4	66.9426	77.1025	89.1247	103.062	118.968	136.897	156.901	179.036	203.355	229.915
0.5	66.294	74.9603	85.41	97.6956	111.87	127.985	146.095	166.253	188.513	212.93
0.6	66.4127	73.689	82.6713	93.4112	105.961	120.372	136.698	154.991	175.305	197.693

0.7	67.1992	73.1867	80.8039	90.1018	101.132	113.945	128.594	145.131	163.609	184.08
0.8	68.5595	73.3567	79.7086	87.6656	97.2783	108.598	121.675	136.563	153.311	171.974
0.9	70.4048	74.1075	79.2912	86.0058	94.3011	104.228	115.836	129.177	144.302	161.263
1	72.6514	75.3528	79.463	85.031	92.1061	100.738	110.977	122.873	136.477	151.839

Table 5: Numerical value of BOD for different value of v and fixed $t = 0.5$

x	$v = 0.1$	$v = 0.3$	$v = 0.5$	$v = 0.7$
0.1	127.372	137.2	148.578	161.637
0.2	118.968	127.372	137.2	148.578
0.3	111.87	118.968	127.372	137.2
0.4	105.961	111.87	118.968	127.372
0.5	101.132	105.961	111.87	118.968
0.6	97.2783	101.132	105.961	111.87
0.7	94.3011	97.2783	101.132	105.961
0.8	92.1061	94.3011	97.2783	101.132
0.9	90.6044	92.1061	94.3011	97.2783
1	89.7122	90.6044	92.1061	94.3011

Table 6: Numerical value of COD at different x and t for $v = 0.5$

$x \backslash t$	0.1	0.2	0.3	0.4	0.5	0.6	0.7	0.8	0.9	1
0.1	267.151	319.156	378.405	445.088	519.396	601.519	691.65	789.984	896.715	1012.04
0.2	255.359	301.119	353.838	413.703	480.902	555.626	638.063	728.407	826.849	933.582
0.3	247.311	287.209	333.786	387.226	447.715	515.441	590.591	673.355	763.923	862.486
0.4	242.61	277.022	317.837	365.236	419.404	480.525	548.785	624.371	707.471	798.275
0.5	240.88	270.172	305.595	347.328	395.554	450.454	512.213	581.015	657.045	740.492
0.6	241.763	266.292	296.684	333.118	375.772	424.826	480.463	542.864	612.213	688.696
0.7	244.916	265.03	290.745	322.235	359.679	403.254	453.139	509.515	572.563	642.465
0.8	250.016	266.055	287.435	314.332	346.918	385.37	429.866	480.582	537.699	601.396
0.9	256.76	269.052	286.433	309.074	337.147	370.825	410.283	455.697	507.244	565.101
1	264.858	273.727	287.434	306.149	330.042	359.285	394.049	434.509	480.839	533.214

Table 7: Numerical value of COD for different value of v and fixed $t = 0.5$

x	$v = 0.1$	$v = 0.3$	$v = 0.5$	$v = 0.7$
0.1	447.715	480.902	519.396	563.644
0.2	419.404	447.715	480.902	519.396
0.3	395.554	419.404	447.715	480.902
0.4	375.772	395.554	419.404	447.715
0.5	359.679	375.772	395.554	419.404
0.6	346.918	359.679	375.772	395.554
0.7	337.147	346.918	359.679	375.772
0.8	330.042	337.147	346.918	359.679
0.9	325.299	330.042	337.147	346.918
1	322.631	325.299	330.042	337.147

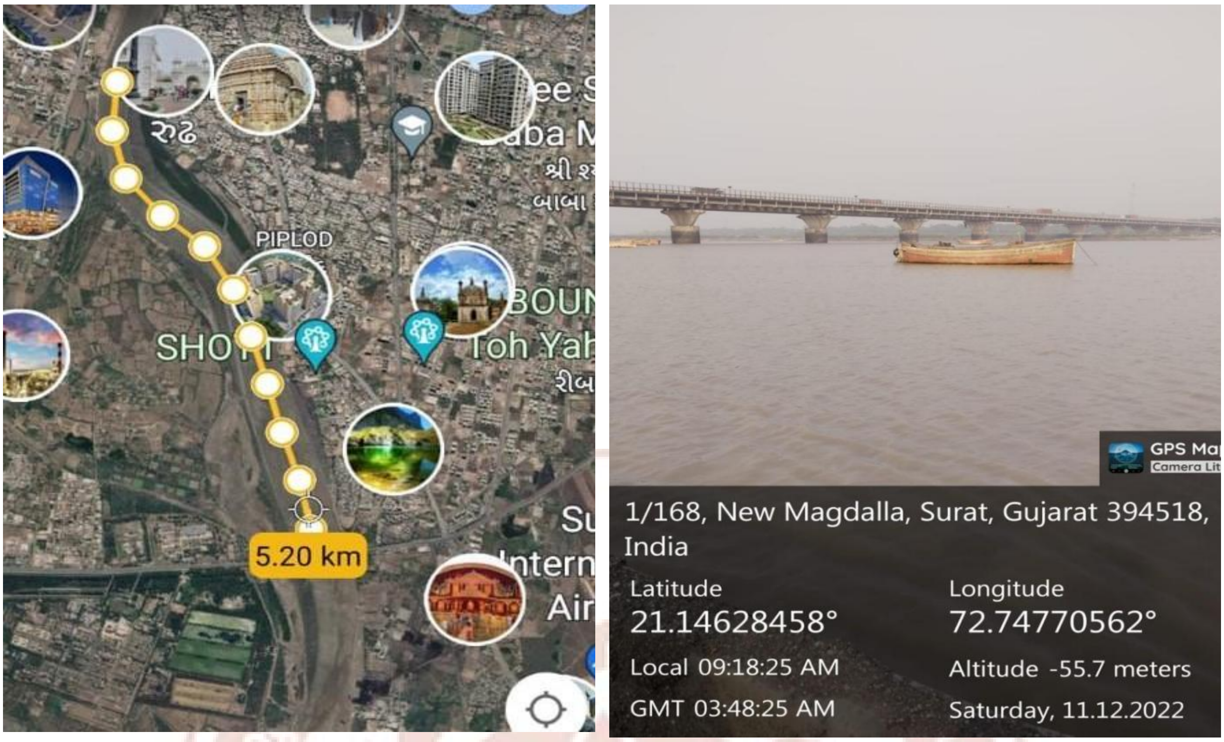

Figure 1: Research area of Tapi river

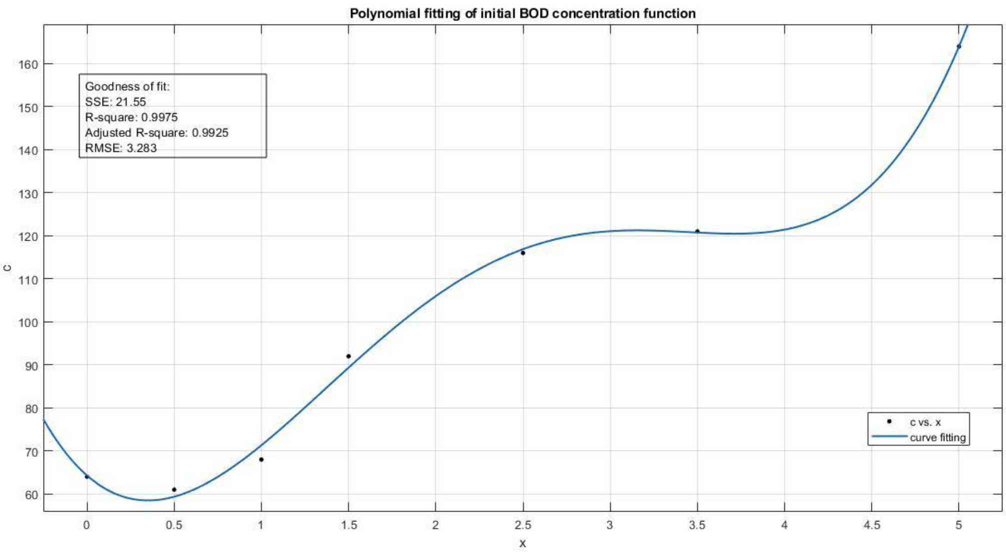

Figure 2: Curve fitting of Initial function of BOD

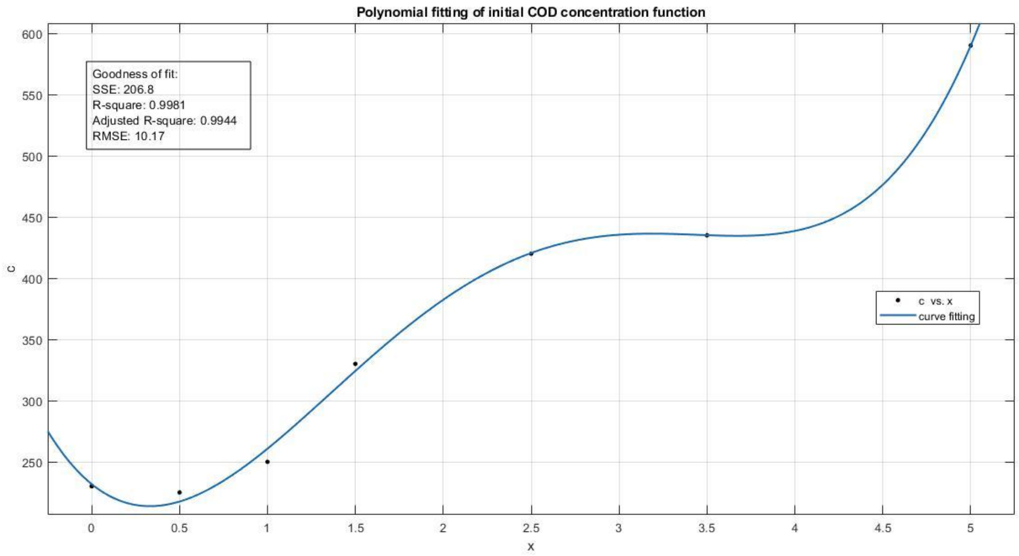

Figure 3: Curve fitting of initial function of COD

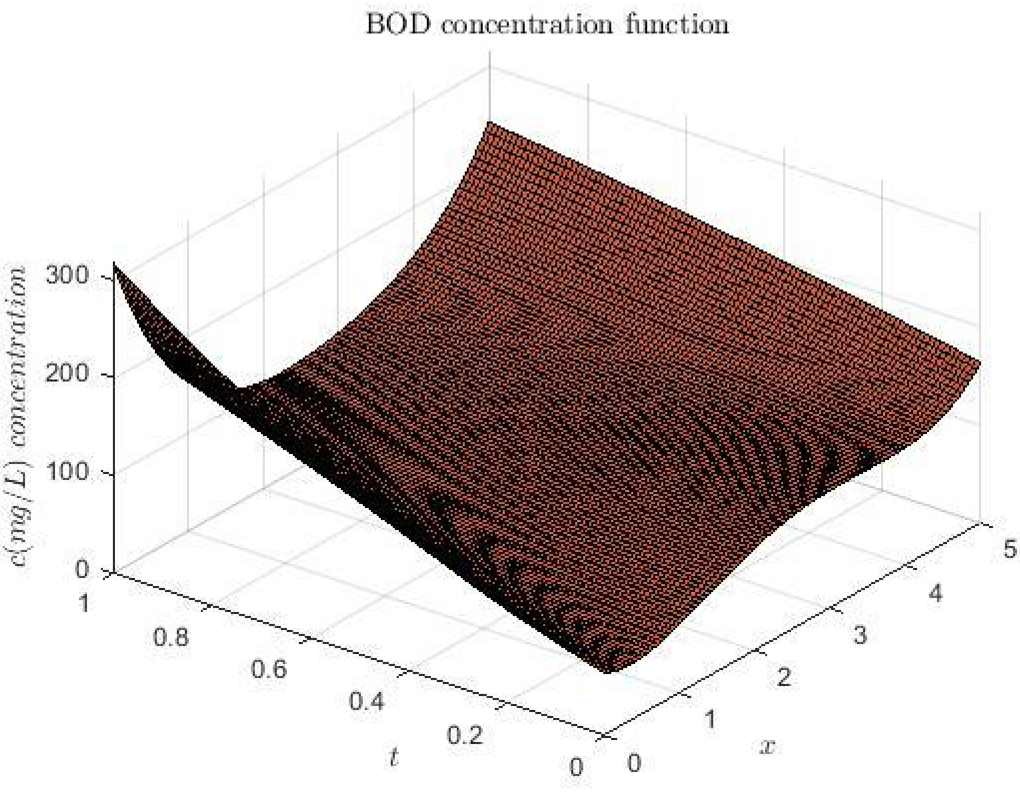

Figure 4: 3D graph of BOD concentration function for $v = 0.5$

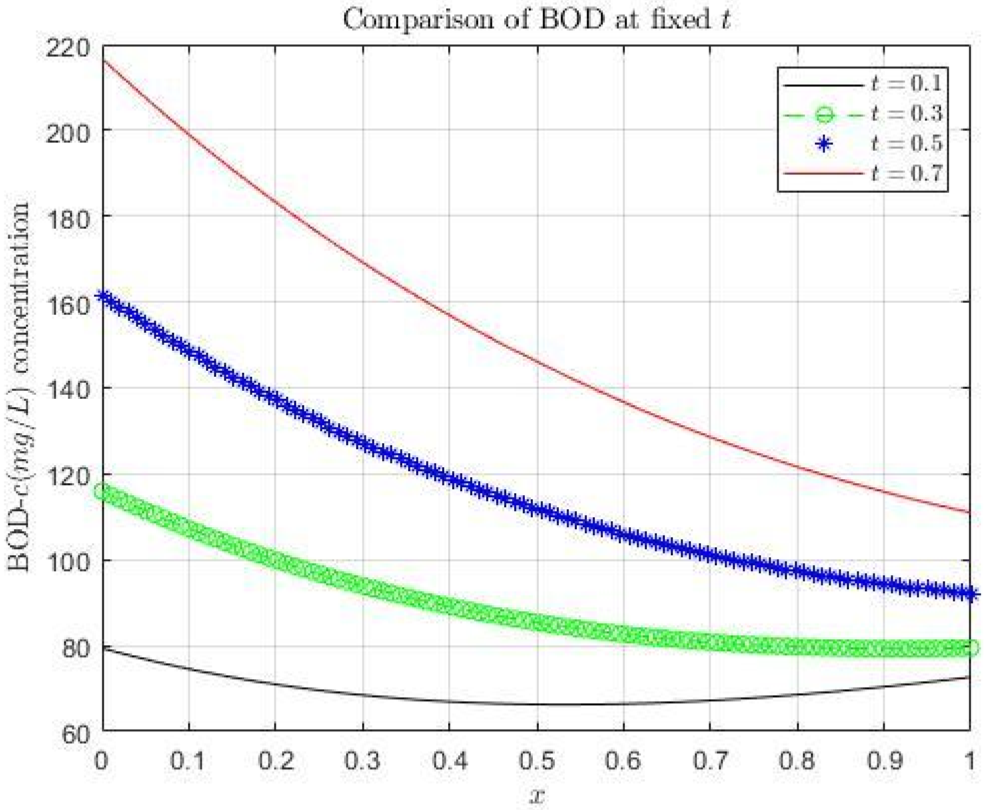

Figure 5: BOD concentration comparison for different value of fixed t

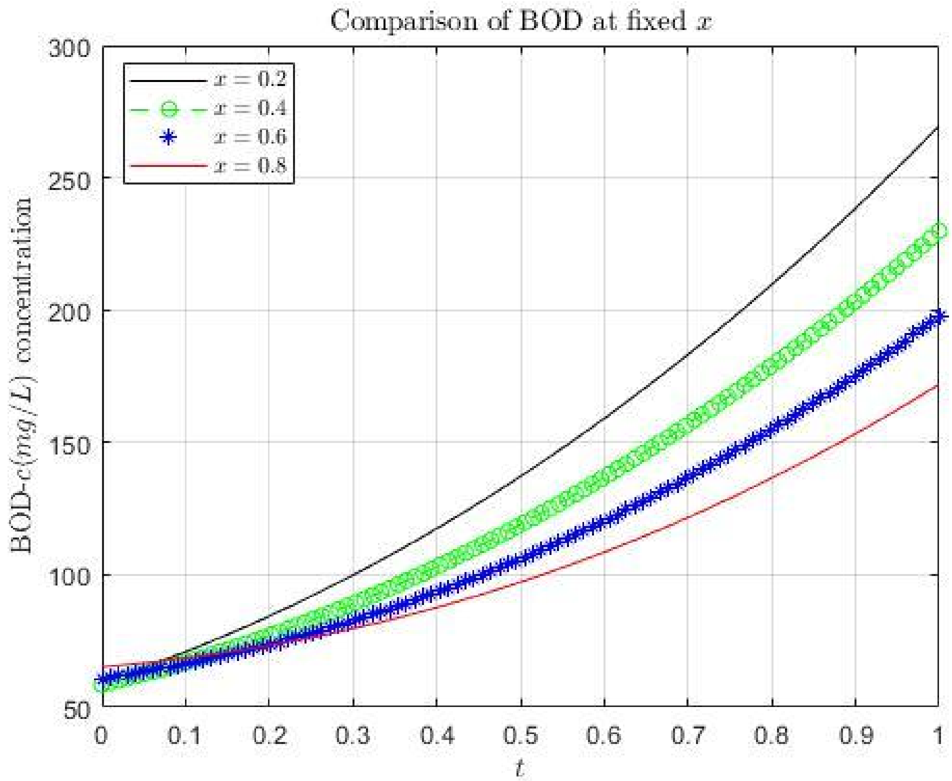

Figure 6: BOD concentration comparison for different value of fixed x

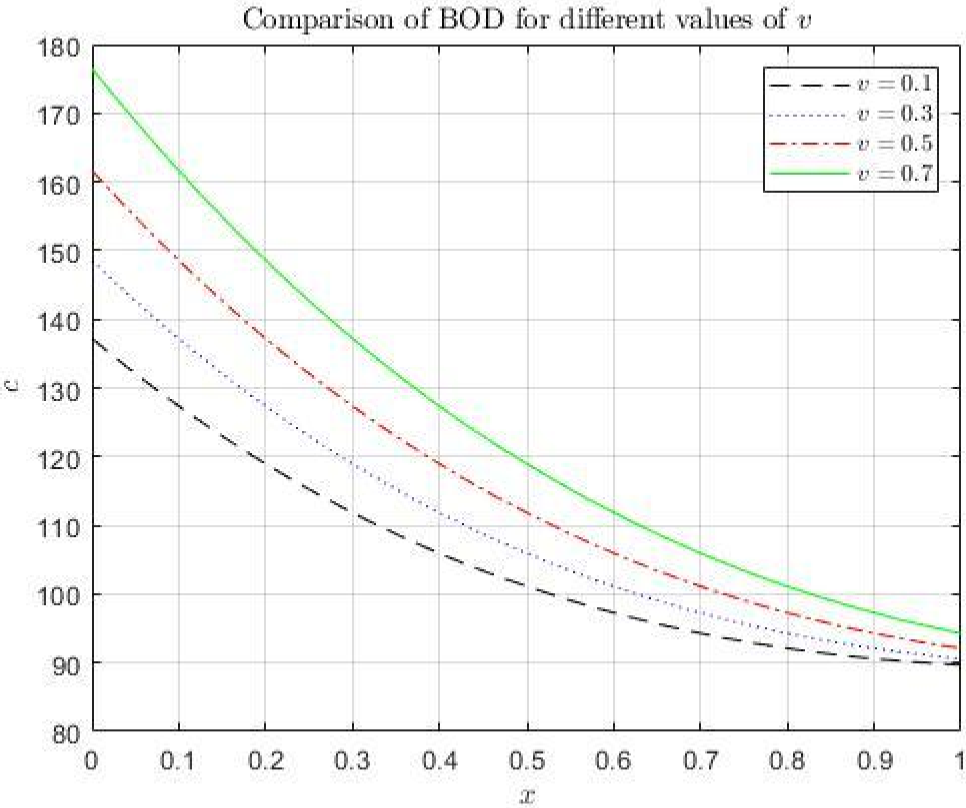

Figure 7: BOD concentration comparison for different value of v **and fixed** $t = 0.5$

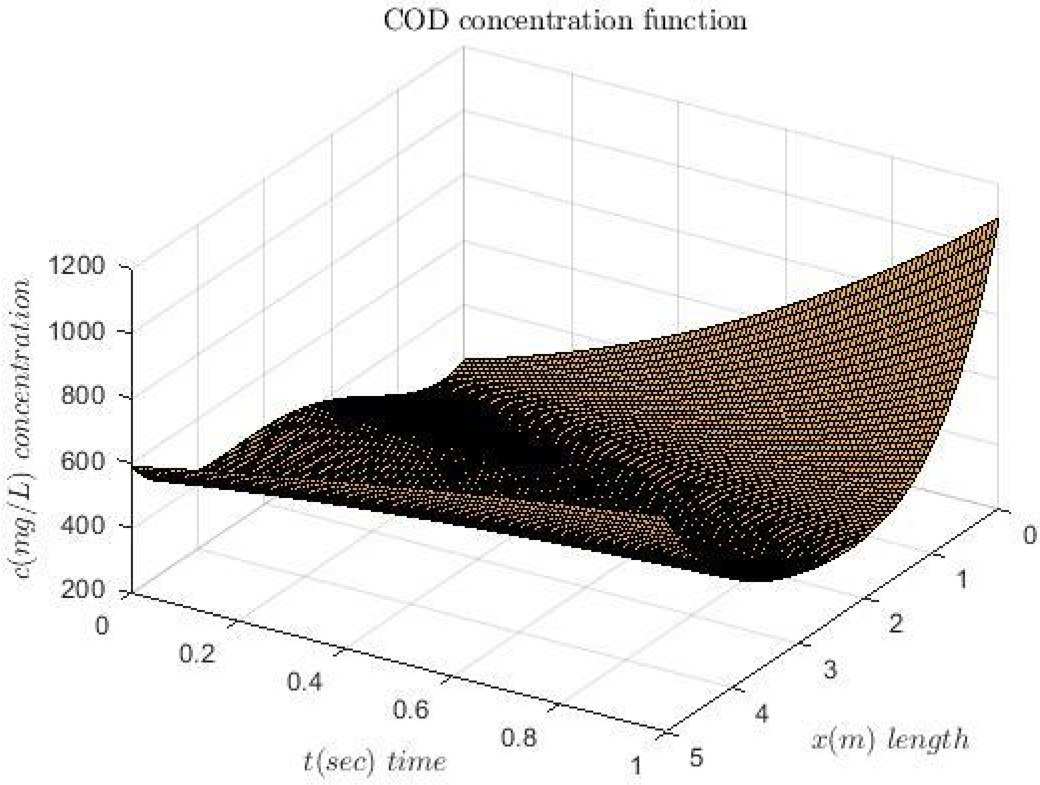

Figure 8: 3D graph of COD concentration function for $v = 0.5$

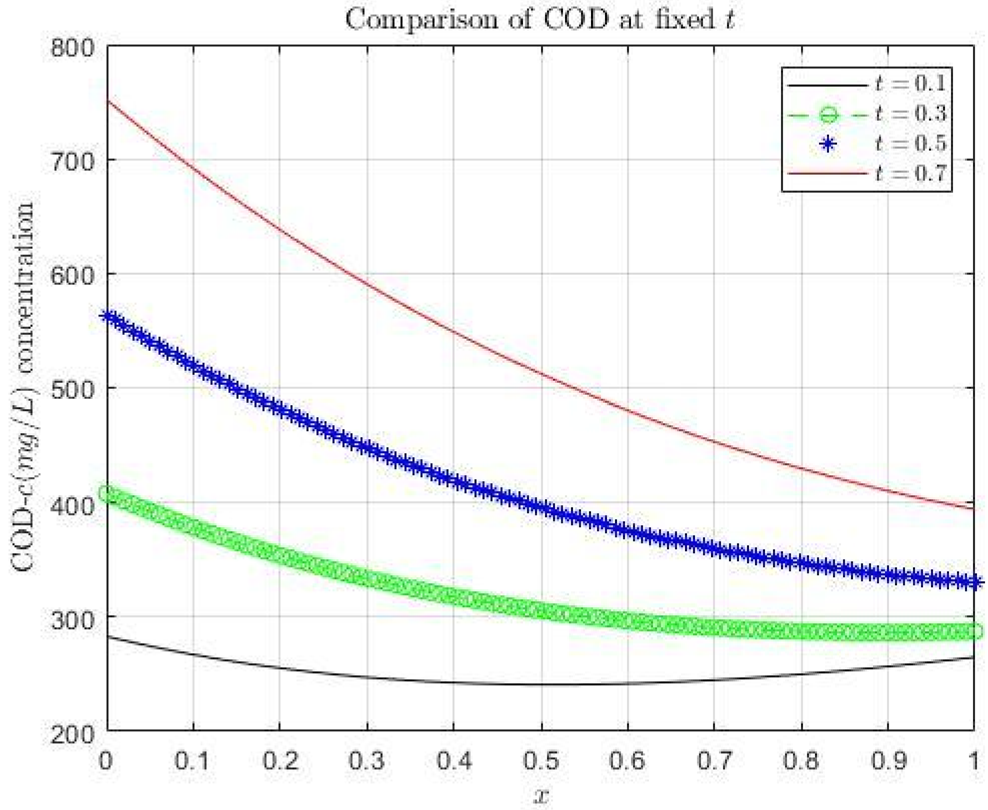

Figure 9: COD concentration comparison for different value of fixed t

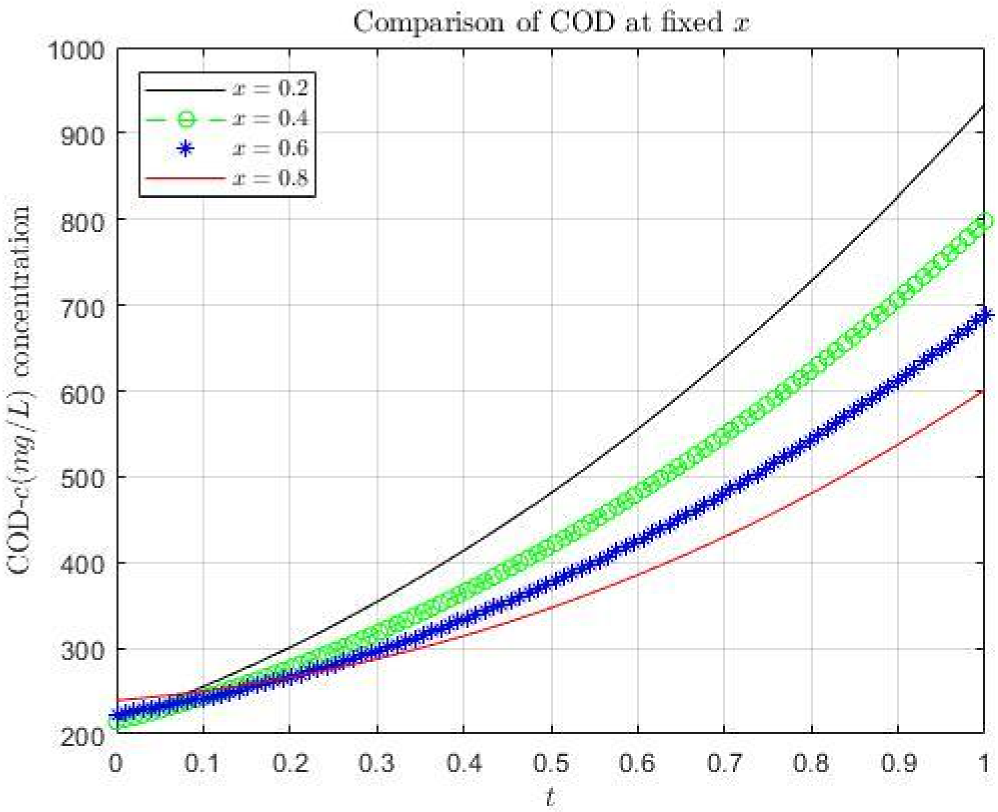

Figure 10: COD concentration comparison for different value of fixed x

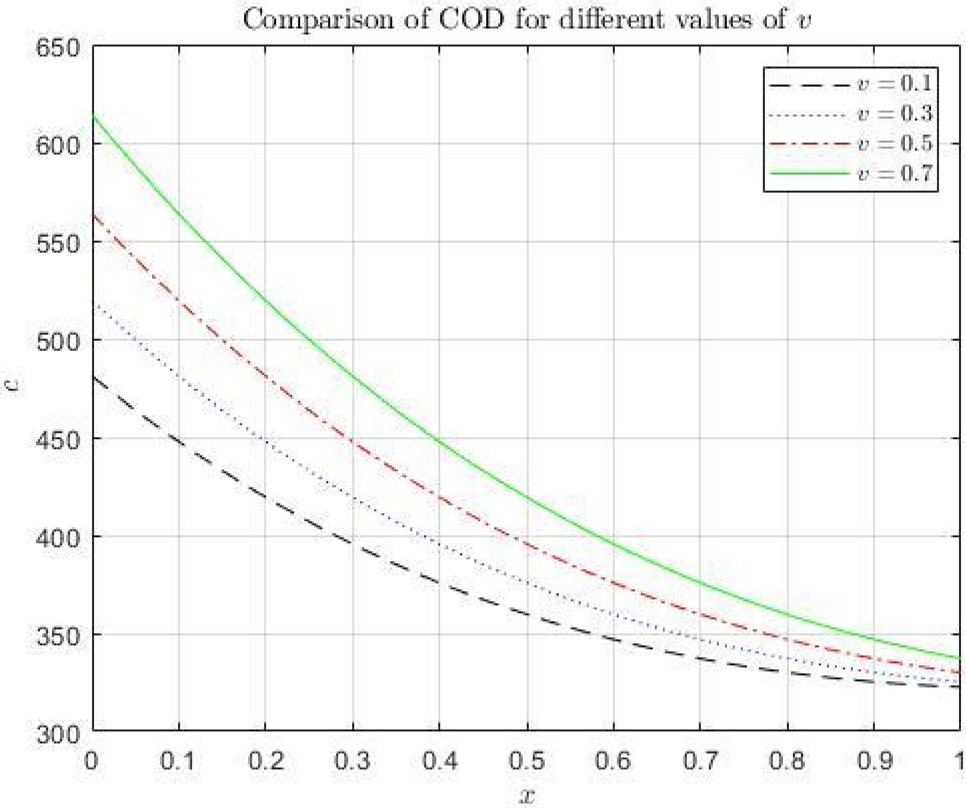

Figure 11: COD concentration comparison for different value of v and fixed $t = 0.5$